

Article

Detection and Classification of Rolling Bearing Defects Using Direct Signal Processing with Deep Convolutional Neural Network

Maciej Skowron ¹, Oliwia Frankiewicz ¹, Jeremi Jan Jarosz ¹, Marcin Wolkiewicz ¹, Mateusz Dybkowski ^{1,*},
Sebastien Weisse ², Jerome Valire ², Agnieszka Wyłomańska ³, Radosław Zimroz ⁴ and Krzysztof Szabat ¹

- ¹ Department of Electrical Machines, Drives and Measurements, Wrocław University of Science and Technology, Wyb. Wyspińskiego 27, 50-370 Wrocław, Poland; maciej.skowron@pwr.edu.pl (M.S.); oliwia.frankiewicz@pwr.edu.pl (O.F.); jeremi.jarosz@pwr.edu.pl (J.J.J.); marcin.wolkiewicz@pwr.edu.pl (M.W.); krzysztof.szabat@pwr.edu.pl (K.S.)
- ² SAFRAN Electrical & Power, Parc d'activité d'Andromède, 1, rue Louis Blériot, 31702 Blagnac Cedex, France; sebastien.weisse@safrangroup.com (S.W.); jerome.valire@safrangroup.com (J.V.)
- ³ Department of Pure Mathematics, Wrocław University of Science and Technology, Wyb. Wyspińskiego 27, 50-370 Wrocław, Poland; agnieszka.wylomanska@pwr.edu.pl
- ⁴ Department of Mining, Wrocław University of Science and Technology, Wyb. Wyspińskiego 27, 50-370 Wrocław, Poland; radoslaw.zimroz@pwr.edu.pl
- * Correspondence: mateusz.dybkowski@pwr.edu.pl

Abstract: Currently, great emphasis is being placed on the electrification of means of transportation, including aviation. The use of electric motors reduces operating and maintenance costs. Electric motors are subjected to various types of damage during operation, of which rolling bearing defects are statistically the most common. This article focuses on presenting a diagnostic tool for bearing conditions based on mechanic vibration signals using convolutional neural networks (CNN). This article presents an alternative to the well-known classical diagnostic tools based on advanced signal processing methods such as the short-time Fourier transform, the Hilbert–Huang transform, etc. The approach described in the article provides fault detection and classification in less than 0.03 s. The proposed structures achieved a classification accuracy of 99.8% on the test set. Special attention was paid to the process of optimizing the CNN structure to achieve the highest possible accuracy with the fewest number of network parameters.

Keywords: induction motor drive; fault diagnosis; rolling bearing faults; artificial intelligence; convolutional neural networks



Citation: Skowron, M.; Frankiewicz, O.; Jarosz, J.J.; Wolkiewicz, M.; Dybkowski, M.; Weisse, S.; Valire, J.; Wyłomańska, A.; Zimroz, R.; Szabat, K. Detection and Classification of Rolling Bearing Defects Using Direct Signal Processing with Deep Convolutional Neural Network. *Electronics* **2024**, *13*, 1722. <https://doi.org/10.3390/electronics13091722>

Academic Editors: Valeri Mladenov and Panagiotis Sarigiannidis

Received: 13 March 2024
Revised: 26 April 2024
Accepted: 28 April 2024
Published: 29 April 2024



Copyright: © 2024 by the authors. Licensee MDPI, Basel, Switzerland. This article is an open access article distributed under the terms and conditions of the Creative Commons Attribution (CC BY) license (<https://creativecommons.org/licenses/by/4.0/>).

1. Introduction

In response to the energy crisis and the need to reduce the negative impact of public transport on the environment, there is now a strong emphasis on the electrification of various modes of transportation, including aircrafts [1]. By replacing conventional internal combustion engines with electric motors, operating costs can be reduced by replacing jet fuel with electricity and reducing maintenance costs for these machines [2]. Despite the high quality of the materials and design methods of electric machines, they are subject to emerging defects. The effect of machine defects can range from reduced functionality to complete failure. Due to the need to ensure the safety of electric vehicles, the diagnosis and prediction of defects in electric machines is an important issue [3]. The correct diagnosis and detection of damage at its initial stage significantly reduce the time of possible machine downtime, avoid harmful, sometimes catastrophic, consequences, and reduce financial losses [4]. The induction motors most commonly used in industrial drive systems consist of many components. Each of these components can fail due to overload, abrasion, electrical, mechanical, and thermal stresses, or as a result of an unbalanced load. According to the results of statistical studies shown in [5,6], rolling bearing damage is the most common recurring failure of electric machines. Bearing fault diagnosis is therefore crucial to ensure

the proper maintenance and trouble-free operation of electric motors. This issue is particularly important for aviation safety, as well as for forecasting and planning maintenance operations [7].

Superior control systems impose several restrictions on the signals used that carry information about the machine's condition. In the case of bearing damage diagnostics, the most commonly used diagnostic signals are vibration [8–10], current [11,12], or acoustic emission [13–15]. A vibration signal is a very good carrier of information and enables the early detection of mechanical damage [16]. Vibration analysis techniques used to detect bearing failures in electric drives are most often divided into four categories: time domain, frequency domain, time–frequency domain, and other methods [17]. Time domain signal analysis includes the analysis of statistical parameters such as RMS, Crest factor, and kurtosis [18]. However, a significant drawback of these methods is their sensitivity to noise and their inability to determine the location of the fault. Frequency domain analysis techniques mainly include fast Fourier transform analysis and envelope analysis [19,20]. However, there are some limitations to these techniques that make them unsuitable for analyzing non-stationary signals. Time–frequency analysis combines the advantages of both methods and includes wavelet transforms, short-time Fourier transform (STFT), and Hilbert–Huang transform, among others [21,22]. However, it should be noted that these methods are more computationally complex, which can lengthen the fault detection process.

The shortest possible time between the occurrence of a defect and its detection is crucial to ensure safety, especially in critical drives. In addition, modern control systems enforce the need for the full automation of the fault detection process, at the same time ensuring a short response time to the appearance of a defect while maintaining high precision in its assessment. Therefore, to meet these requirements, but also to increase the reliability of diagnostic systems, artificial intelligence techniques are increasingly used [23]. Artificial neural networks are now a very good tool to partially replace humans in the decision-making process, based on signal analysis [10,24], allowing them to automate and maintain the diagnostic process [25,26].

The most widely used neural structure in diagnostic applications is the multilayer perceptron (MLP), whose use and good precision performance have been described in [27–29], among others. These networks perform the primary function of learning data approximation and perform well in simple diagnostic tasks based on signal preprocessing. Other widely used types of shallow neural networks are self-organizing Kohonen maps (SOM) [30,31], networks with radial activation functions (RBF) [32], or recurrent structures [33]. However, these solutions base their operation on the extraction of classical symptoms, which implies the use of analysis methods whose limitations have been mentioned above.

A natural development step in automating the decision-making process of diagnostic systems was to use methods that would allow the direct use of the diagnostic signal. One solution with good results was the use of deep neural networks [10,34–37]. The structure of deep neural networks is based on the use of many different neural layers [15], each of which introduces a certain level of abstraction by extracting successive features from the data coming from the previous layer, starting from the input layer [38,39]. This also makes use of features extracted from processed diagnostic signals as an input for deep network work [10,40]; however, an important advantage of deep networks is their ability to extract features directly from the diagnostic signal and their ability to process them for appropriate classification [38,39,41,42].

The most widely used deep learning network structures are autoencoders [43], long short-term memory (LSTM) [7], and convolutional neural networks (CNNs) [36,44–46]. Compared to the shallow structures mentioned above, CNNs show higher accuracy when operating directly on the diagnostic signal presented in the form of multidimensional arrays or vectors [38,45], further reducing the time of the diagnostic process [36,37]. CNNs also provide automatic symptom extraction, reducing the role of an expert in the diagnostic process. Due to the direct processing of diagnostic signals, fault response times are many

times faster than known classical detection methods. Furthermore, the technique performs well in detection during steady-state and transient conditions, which is extremely important for modern drive systems. The topic of bearing damage detection using CNNs with a direct diagnostic signal, such as vibrations, has been addressed in publications [10,15,46,47], among others. However, in this paper, the authors used signals for a larger number of degrees of different damage, which allows an increase in the sensitivity of the neural structure for the initial stage of damage [15].

In addition, in the article [46], time–frequency analysis was used to develop the input matrix of the network. This fact adversely affects the diagnostic process due to the significant computational load of the applied combination of continuous wavelet analysis (CWT) and a deep convolutional network. Furthermore, the signal acquisition time declared in [46] is 0.5 s, which is 25 times longer than the time presented in this article. Also noteworthy is the very elaborate structure of the fully connected layer presented in [46], which is not justified, especially in the context of the initial symptom extraction applied using CWT. The article [47] proposed an approach based on the analysis of the vibration signal in the time domain. Feature extraction was enhanced by the statistical analysis of vibration samples contained in the measurement vector. However, the disadvantage of the described approach is the use of a ready-made AlexNet structure without taking into account the possibility of optimization. The CNN structure presented in [47] contained more than 2.5 billion parameters adapted to the training process. In addition, the transition between convolutional layers containing more than 3.3 million parameters and a classifier containing more than 2.6 billion parameters was not protected against a loss of generalization. It should be noted that the lack of an optimization algorithm between the layers of the feature detector (convolutional layers) and the layers of the classifier (fully connected layers) results in an excessive dependence of the state of one neuron on the others. In the approach proposed in this article, a structure with 64 thousand parameters is used. In addition, a dropout layer [10,38] and stochastic network training methods were used to avoid a loss of generalization ability.

Recognizing damage at a possible early stage is extremely crucial for critical propulsion systems (aviation) given the early prediction of required maintenance work to ensure system reliability [10]. Due to the application of ready-made neural structures with an excessive number of neural connections presented in the literature, this article presents the optimization of the CNN structure to maximize the accuracy of performance and minimize the required time and computational resources. Due to the crucial role played in modern diagnostic systems by the immunity of the solution to external disturbances [45] and the stability of the system's operation, it is important to optimize the neural structure that is a key element of the diagnostic application [41]. A reduced number of network parameters translates directly into the ability to implement the solution and response time to an emerging defect. So far, this issue has not been discussed in the literature concerning rolling element-bearing diagnostics, so this article describes a study showing the possibility of deep network optimization for diagnostic tasks.

2. Rolling Bearing Damage—Analysis of the Fault Detection Problem

2.1. Extraction of Damage Symptoms Using Spectral Analysis

When damage occurs on the surface of any of the bearing elements, each time one of the rolling elements rolls through the damaged area, a brief impulsive force is generated that causes the bearing to vibrate. If the speed is constant, these pulses occur periodically. Periodic changes in the vibration signal resulting from rolling bearing defects provide excellent information to determine the nature of the damage. The analysis of the impact of periodically occurring changes in signals, which can be understood as the evaluation of the contribution of damage-related features to the measured signal, is now mainly implemented using the fast Fourier transform. With the FFT, it is possible to assess the trend of amplitude changes associated with rolling bearing defects that occur at specific

frequencies of the spectrum. For a ball bearing in which the inner race rotates and the outer race is stationary, the characteristic frequencies for each type of defect are as follows [16,48]:

$$f_C = 0.5 \cdot f_r \cdot \left(1 - \frac{d \cdot \cos \vartheta}{D}\right), \quad (1)$$

$$f_B = \frac{D}{2d} \cdot f_r \cdot \left(1 - \left(\frac{d \cdot \cos \vartheta}{D}\right)^2\right), \quad (2)$$

$$f_O = \frac{N_B}{2} \cdot f_r \cdot \left(1 - \frac{d \cdot \cos \vartheta}{D}\right), \quad (3)$$

$$f_I = \frac{N_B}{2} \cdot f_r \cdot \left(1 + \frac{d \cdot \cos \vartheta}{D}\right), \quad (4)$$

where f_r is the rotational frequency, f_C is the frequency associated with cage failure, f_B is the frequency associated with rolling element failure, f_O is the frequency associated with outer race failure, f_I is the frequency associated with inner race failure, N_B is the number of rolling elements, D is the pitch diameter of the bearing, d is the diameter of the rolling element, and ϑ is the operating angle of the bearing.

2.2. Methodology of the Conducted Experimental Research

The test bench (Figure 1) used for the experimental tests consisted of an *INDUKTA Sh90L-4* induction motor (Celma Indukta S.A., Cantoni Group, Cieszyn, Poland), which was mechanically coupled to a *PZB b44b* DC external motor. Load control is achieved by varying the motor arm current at a constant excitation current. A triaxial accelerometer type *4506-B-003* placed on the counter-drive side and a uniaxial sensor type *4514-001* placed on the drive side were used to measure mechanical vibrations. The measured diagnostic signal in the form of a voltage signal was fed directly to a National Instruments measurement card. A single measurement was performed in 10 s with a sampling rate of 50 kHz, which ensured a high resolution of the spectrum. Based on the measurements performed on the object, the measured signal was measured and processed. For this purpose, a measurement and diagnostic application was developed in the *LabVIEW 2019* and *MATLAB 2022a* environments.

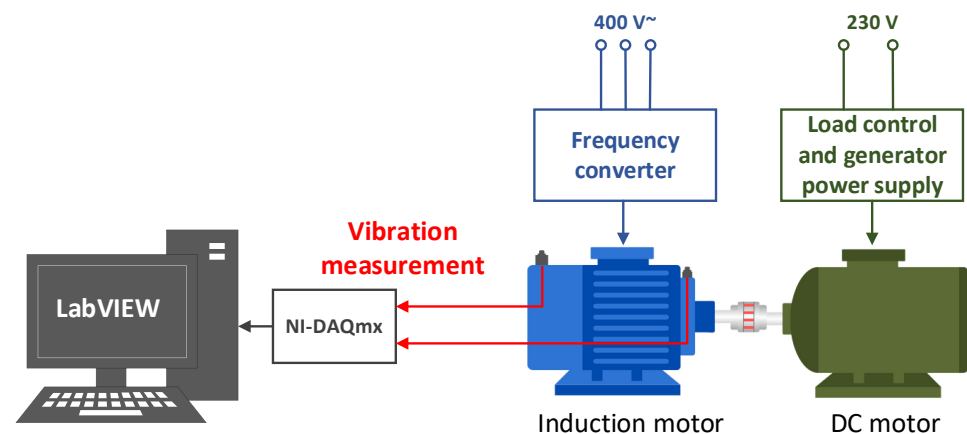


Figure 1. Diagram of the test bench.

Two bearings from *SKF 6205-Z* are mounted in the engine under study, the design dimensions of which are shown in Table 1. During the tests, the damaged bearings were mounted on the counter-drive side. The classification and photos of all the damages tested are shown in Figure 2. The following types of damage were investigated for the outer and inner races:

- Longitudinal scratch at a length of 3 mm;
- A spot indentation 1 mm deep;

- Two spot indentations 1 mm deep;
- Transverse scratch.

Table 1. Dimensions of construction of the *SKF 6205-Z* bearing.

Bearing Element	Description	Value	Unit
Diameter of the rolling element	d	8	mm
Bearing pitch diameter	D	39	mm
Number of rolling elements	N_B	9	-
Bearing operating angle	ϑ	0	°

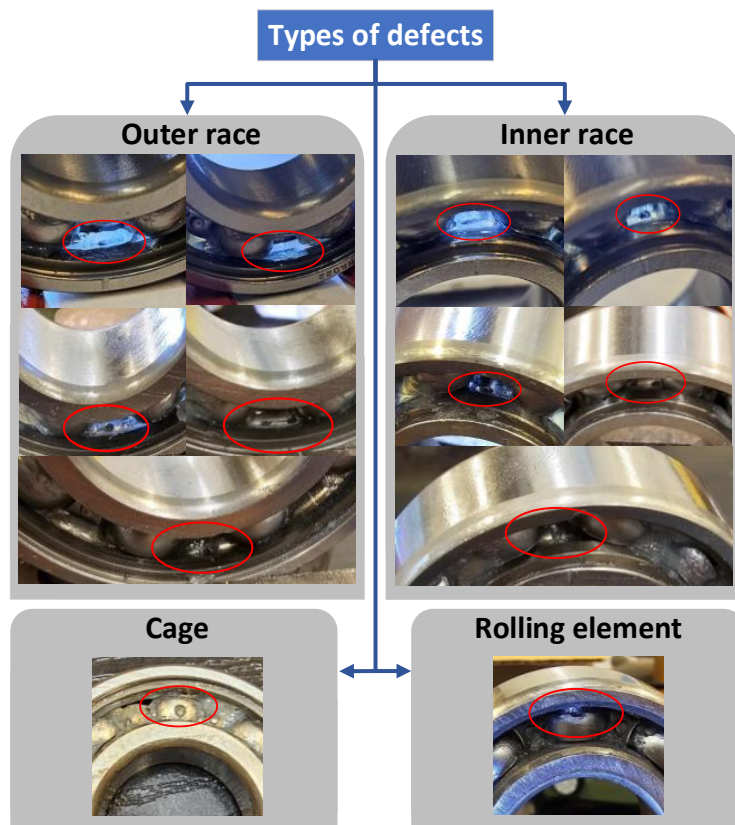


Figure 2. Classification of damage to the bearing analyzed.

The conduct of tests for different stages of damage made it possible to assess the effectiveness and precision of the proposed solution for the initial and advanced stages of the mechanical degradation of the bearing. For each of the types of damage analyzed, measurements were carried out for the operation of the induction motor under different load conditions (in the range of $0-T_{LN}$). Additionally, to compare the effect of an external machine mechanically coupled to the motor under study, measurements were made in the absence of this coupling. This eliminated the situation in which the auxiliary machine asymmetry was transferred to the test machine. To analyze the impact of individual rolling bearing failures, a spectral analysis of mechanical vibrations was carried out. The results of the analysis are presented in the next section.

2.3. Spectral Analysis of Mechanical Vibration Signal

The algorithm to calculate the envelope of a signal involves averaging it with a bandpass filter with an appropriately selected bandwidth, then using the Hilbert function, an analytical signal is calculated, the absolute value of which is the envelope signal [49].

The band selection was determined by the technique provided by the bearing manufacturer (Bruel&Kjaer, Nærum, Denmark). For the induction motor used in the research

work, used to install the bearing node described in the manufacturer's documentation, the frequency was determined experimentally as 1600 Hz. It should be emphasized that the bandwidth was individually determined for each machine based on experimental measurements of the natural frequency of the bearing node. By filtering the signal and averaging it, it is possible to remove interference that can interfere with the extraction of the symptoms of the damage under study.

A comparison of the frequency spectrum of the envelope for an undamaged bearing and four different types of damage at a load equal to half the rated load and a rotational speed of 1450 rpm is shown in Figures 3–6. For each of the cases studied, it is possible to extract the characteristic frequencies of the damage. However, during the frequency analysis of the signal, the accuracy of the analysis is affected by the resolution of the spectrum under study. This parameter depends on the number of samples of the measured signal, that is, the sampling frequency and the measurement time. To increase the resolution of the spectrum at a constant sampling frequency, it is necessary to increase the measurement time. However, an important limitation is that the measurement must take place under constant load conditions and supply voltage frequency (steady state). This makes signal analysis methods based on the fast Fourier transform unsuitable for applications in which the operating conditions of the drives under testing change dynamically [50].

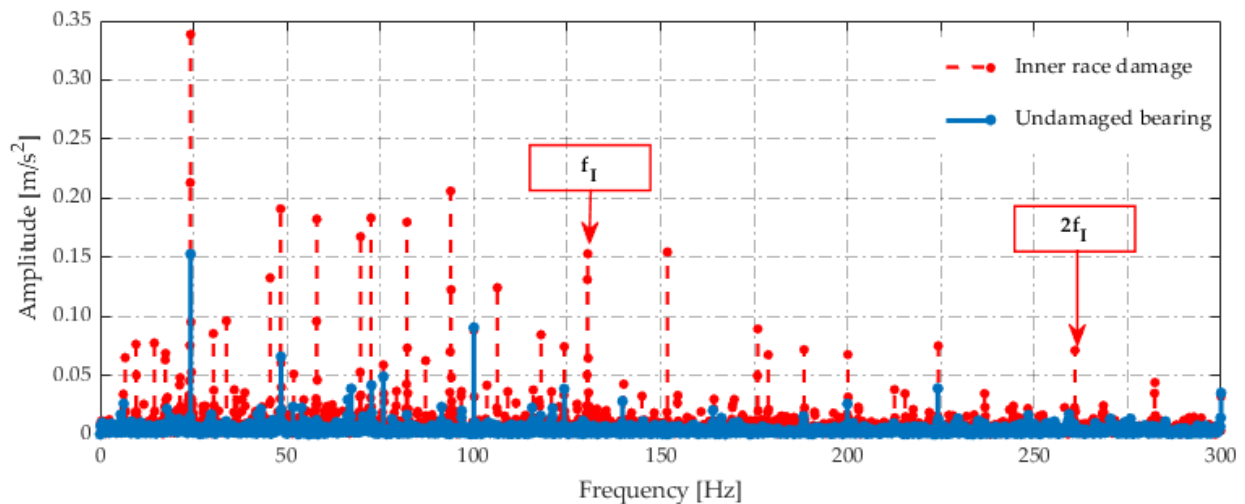


Figure 3. Envelope spectrum—undamaged bearing and inner race damage, $T_L = 0.5T_{LN}$, $f_s = 50$ Hz.

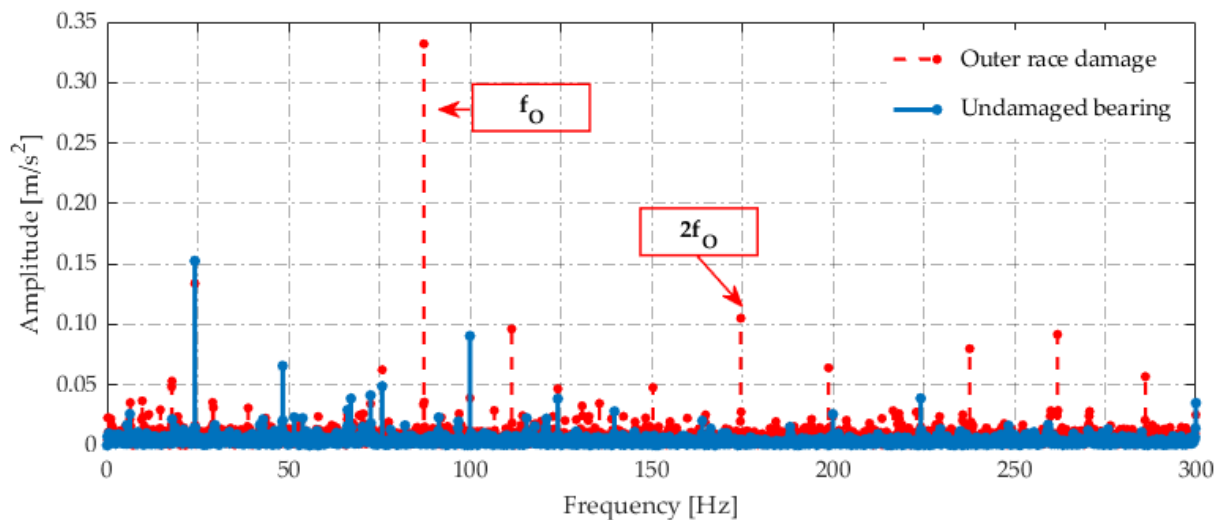


Figure 4. Envelope spectrum—undamaged bearing and outer race damage, $T_L = 0.5T_{LN}$, $f_s = 50$ Hz.

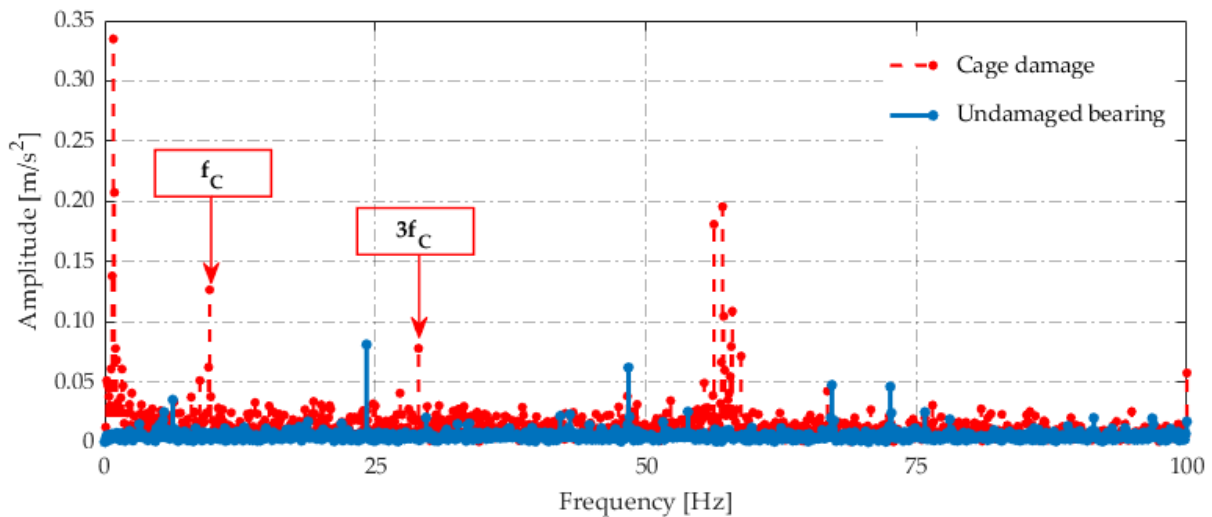


Figure 5. Envelope spectrum—undamaged bearing and cage damage, $T_L = 0.5T_{LN}$, $f_s = 50$ Hz.

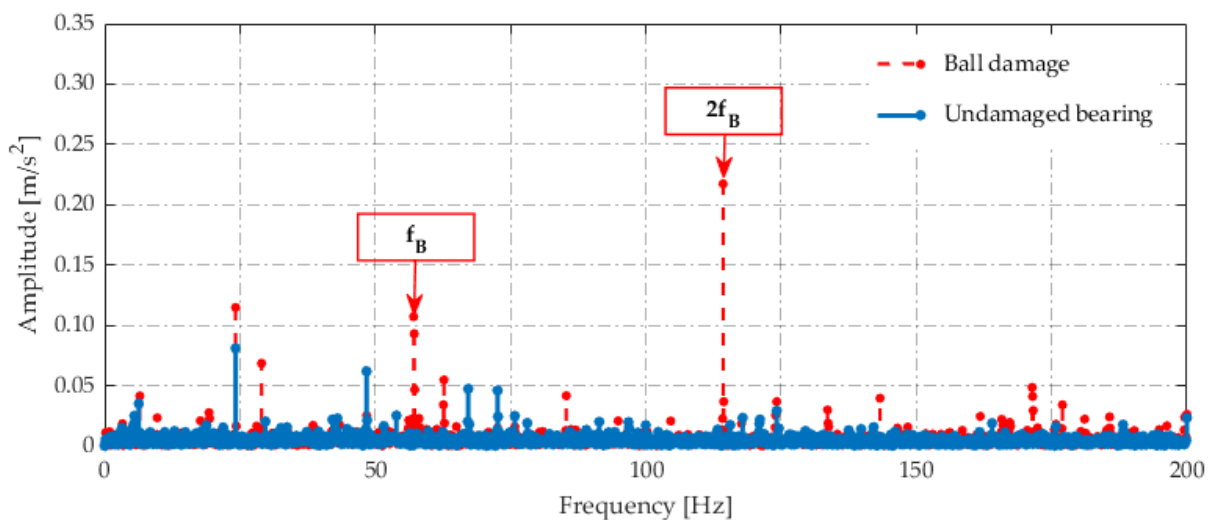


Figure 6. Envelope spectrum—undamaged bearing and rolling element damage, $T_L = 0.5T_{LN}$, $f_s = 50$ Hz.

3. Bearing Fault Detection and Classification System Based on a Convolutional Neural Network

Convolutional neural networks (CNNs) are currently being used in an increasing number of applications due to their high precision in automatic data analysis. Initially, they were used mainly in image processing, but with the appropriate signal transformations, they are increasingly finding widespread use in electrical machine diagnostics, among other applications. With the ability to directly analyze diagnostic signals, CNNs are defining increasingly abstract sets of features, enabling the generation of high-level patterns and, ultimately, allowing appropriate signal classification. The performance of the structure is strongly dependent on many factors, including the input signal, the selected number of layers, and appropriately selected hyperparameters, which affect not only the accuracy of the structure's performance, but also the processing time of the input information, so optimizing the structure and the parameters of the training process is an important step in the development of a diagnostic application.

3.1. Development of Deep Network Input Information

The operation of the convolutional structure forces the processing of input information in the form of a two- or three-dimensional matrix (Figure 7). Therefore, the appropriate processing of diagnostic signals is aimed at making optimal use of the properties of CNN.

The diagnostic approach proposed in the article used signals recorded from a triaxial sensor. Given this, the collected data included three time series for the X, Y, and Z axes, respectively. In each measurement series, 1000 samples were recorded, which corresponded to a signal acquisition time of 0.02 s. The vectors were then transformed into a 25×40 matrix. The use of such a matrix shape allows the use of filters in convolution layers with small dimensions. In addition, the developed structure does not require the use of the zero-padding technique. Thus, the entirety of the detected simple and higher-order features is taken into account in the final classification.

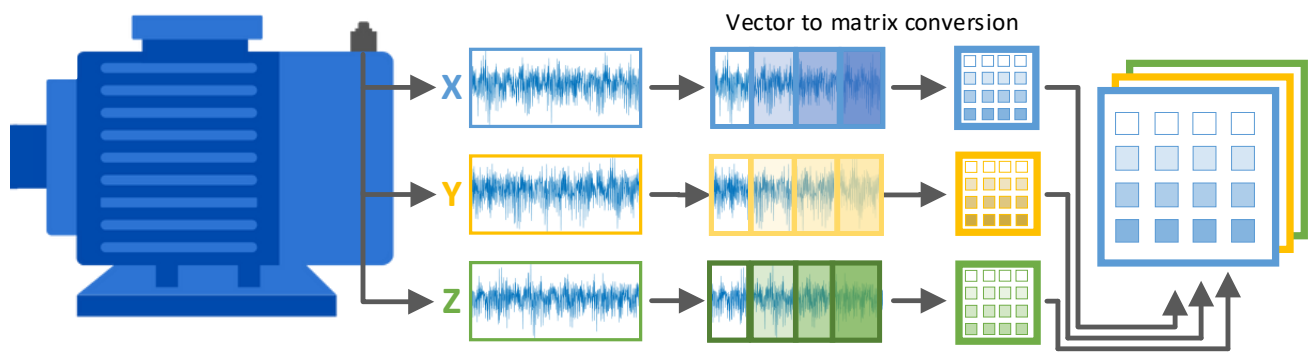


Figure 7. Preparation of the CNN input matrix: idea diagram.

An equally important aspect of preparing the signals for input to the CNN was the normalization of vectors containing samples of the measured mechanical vibrations. Overestimated values affect the updates of the network weights and significantly increase computation time, and thus training time. This fact is due to very large gradient jumps known in the literature as an “exploding gradient.” In the final stage of processing, the data were combined into a 3D matrix, and in this form, they were fed to the input of the structure. In total, 19,500 samples were collected (1500 cases for each of the 13 damage categories). The developed data set was randomly divided into three packages (keeping the same number of samples in the considered class):

- Training package used in the training process,
- Validation package used to analyze the stability of the learning process and avoid loss of generalization (analysis of learning curves),
- Testing package used to determine the additional precision coefficient of the network (after the training process).

Table 2 shows the exact distribution of data allocated to the training, validation, and testing processes for each piece of damage under investigation, where the sets were chosen to contain different loads, from 0 to nominal in 20% increments. This was done to ensure the good generalization of the network being trained.

Table 2. Summary of the number of samples for each type of damage and process.

Type of Fault	Number of Samples (Cases)		
	Training	Validation	Test
No fault	500	500	500
Inner race	2500	2500	2500
Outer race	2500	2500	2500
Rolling element	500	500	500
Cage	500	500	500
Summary	6500	6500	6500

3.2. Development of Deep Network Structure

CNNs are steadily gaining popularity due to their ability to use raw data in the classification process. Their architecture in general usually includes layers such as a convolution layer, which is responsible for converting the provided data into new information with a higher degree of abstraction, a pooling layer, which is responsible for selecting the information created in the convolution layer, thus leading to a reduction in the dimension of the data, and a fully connected layer, which is ultimately responsible for classifying the input data based on the features detected by the convolution layers. However, the proposed CNN structure also includes additional layers to ensure the restoration of non-linear dependencies and the stabilization of the training process (Table 3).

Table 3. Parameters of the convolutional neural network structure used.

Parameter Name	Parameter Value	Structure Scheme
Number of convolution layers	3	
Number of filters	20-40-60	
Dimension of filters	5 × 5	
Stride	(1 × 1), (2 × 2), (2 × 2)	
Number of normalization layers	3	
Value of the coefficient ε	0.001	
Number of activation layers	3	
Activation function	ReLU	
Number of pooling layers	3	
Pooling method	maximum	
Window size	3 × 3	
Stride	(1 × 1), (2 × 2), (2 × 2)	
Dropout probability	0.5	
Number of fully connected layers	2	
Number of fully connected neurons	(60), (13)	

- Convolution layer: Consisting of a set of different filters, each of which is responsible for extracting a different selected feature (by tuning the window parameters). The filter window determines the output features using a convolution operation of the filter g and the set h to which the filter is applied:

$$C = g[x, y] * h[x, y] = \sum_i \left(\sum_j (g[i, j] \cdot h[x - i, y - j]) \right) \tag{5}$$

- where C is the resulting matrix of higher-order features found with the selected filter.
- Batch normalization layer: Used to speed up the network training process and increase accuracy by reducing the internal variation of the data range. During the training process, the mean and standard deviation are calculated for each mini-packet and provide the normalization of the convolution layers' weighting factors to the 0–1 range.
- Activation function: Ensures that the network correctly reproduces non-linear relationships. For CNNs, the most commonly used activation function is the Rectified Linear Unit (ReLU). ReLU is most commonly used because of the simplicity of calculating both the result and the derivative, which accelerates the training process.
- The pooling layer: Determines which information is useful in context to evaluate the class of the input matrix. In addition, it allows the dimensionality of the data to be reduced, leading to lower computing power requirements and improved generalization capabilities.
- Dropout layer: involves removing selected neural connections at the input of the first fully connected layer, which allows one to speed up the training process and, above all, to make the state of individual neurons independent of each other (improving generalization ability).

- Fully connected layer: Is responsible for determining the contribution of matrix features to the final evaluation of category membership. The most common way to use the final classification is to use the softmax function, which determines the probabilities of a given input belonging to each of the analyzed classes.

3.3. Convolutional Neural Networks—Training Process Hyperparameters

One of the most commonly used algorithms in the training process is stochastic gradient descent (SGD), which is characterized by calculating an averaged gradient for individual mini-batches of learning data. However, a limitation of the SGD algorithm is the high variance of the gradient update, which can lead to slow convergence (getting stuck at the local minimum or the so-called saddle). A popular enhancement to this algorithm is the addition of a “momentum” factor, which introduces gradient-matching adaptation by referring to the history of gradient changes in earlier learning iterations (Table 4). This extension is referred to as stochastic gradient descent with momentum (SGDM), which allows not only for the better convergence of the network learning process, but also for bypassing local minima of the objective function. According to the SGDM algorithm, in each iteration, the average gradient was determined for 90 randomly selected samples (mini-batch) from the entire training data set. The number of iterations was selected so that all training data samples were presented at each epoch. Moreover, after the end of each epoch, the mini-batch was shuffled, thanks to which the gradient was averaged based on different samples. Updates to network parameters are based on the following formula.

$$\theta_{t+1} = \theta_t - v_{t+1} \quad (6)$$

where

$$v_{t+1} = \mu \cdot v_t + \eta \cdot \nabla J(\theta_t) \quad (7)$$

and where θ_t is the network parameters in step t , ∇J is the gradient of the objective function, η is the learning rate, v_t is the velocity vector in step t , and μ is the momentum factor.

Table 4. Parameters of the CNN training process.

Parameter Name	Parameter Value
Learning method	SGDM
Momentum value	0.95
Initial value of learning rate	0.002
Number of learning epochs	500
Decreasing period	10
Input matrix size	25×40
Execution environment	GPU
Mini-batch size	90
Size of training data set	6500
Number of considered classes	13

4. CNN-Based Diagnostic System for Bearing Faults

Fault diagnostic systems that use direct signal processing are characterized by an extended structure compared to classical solutions. The extensive network architecture enables the extraction of the characteristics of the input matrices for assignment to one of the damage categories considered. Deep neural networks are distinguished by their lack of formal rules for the selection of network hyperparameters, so these structures in diagnostic applications are often too extensive. Therefore, it is important to optimize the number of neuronal connections. Of key importance for a CNN is the selection of the number of filters that perform the function of extracting the features of the input matrix. The applications of deep neural networks in electrical motor diagnostics encountered in the literature are characterized by the large number of filters that significantly increase the number of parameters required for adaptation during the training process. Another

approach described in the literature is the use of pre-trained structures developed for image recognition tasks such as AlexNet, ResNet, and GoogLeNet. The result of the elaborate structure is a significant lengthening of the process of the adaptation of weighting factors of convolutional layers. To eliminate this phenomenon, the research assumed a minimum precision threshold of the network with the selection of parameters dedicated to the development of the smallest possible structure that achieves the assumed efficiency threshold. Moreover, it is important to adapt the structure of the deep network to the changing conditions of the training process such as available data packets. Only in the absence of a strict dependence on the precision of the diagnostic system on the size and quality of the available information is it possible to ensure correct fault detection [51]. During the experimental study, structures with three convolutional layers and one classifier layer were analyzed. The process was limited to changing the number of filters of three convolutional layers. Optimization included the amount of information that went to the classifier, which allowed the input matrix to be properly assigned to a class. A total of 125 deep convolutional network structures were analyzed (changing the number of filters in each layer from 20 to 100 with a step of 20). For each of the analyzed structures, the number of neural connections, the number of parameters required for tuning, as well as the training time, and the final precision achieved for the test data were determined. To analyze the accuracy of the training process, the impact of available training data on the precision of the bearing damage detection system was determined. Research included the use of variable sizes of training samples from the available data package in the process of adapting the weight coefficients of the network. To show the influence of the amount of information (λ coefficient: training data size/training packet in percent) on the effectiveness of fault classification, the same CNN structure was used in each case. The research used a range of coefficient changes from 5% to 49% with a 2% step of change. The results of the conducted analyses are presented in Figure 8b. The test results are shown in the dependence of the network's accuracy on the number of its parameters in the figure below. As can be seen in Figure 8a, increasing the number of parameters does not necessarily translate into an increased accuracy of network performance. In addition, outlier samples are observed which, despite an increase in the number of neural connections, did not result in correct adaptation. Nevertheless, the trend of changes allows a limited increase in the precision of the damage class assessment. This means that the choice of network parameters should be a compromise between the number of parameters and the assumed minimum precision of the detection system. Therefore, in further studies, out of the 125 structures analyzed, those selected were the ones that met the assumed quality criterion with the lowest possible number of neural connections. Moreover, the research has shown that the use of a training data package containing over 25% of available samples provides less than a 99% level of damage classification precision (Figure 8b). This means that despite the available information obtained as a result of a short acquisition time, it is possible to develop sufficient sets of training data. Moreover, the high efficiency for the variable conditions of the training process (available data) confirms the high quality of the automatic extraction of damaged features directly visible in mechanical vibration signals.

The classification performance was determined based on a data set that contained samples for 13 categories (Appendix A) with a total dimension of 6500 cases. Based on the results of neural computations for 125 CNN structures, those that met certain assumptions regarding the precision of damage classification were selected (Table 5).

The juxtaposition of the obtained results presented in Table 5 allows us to observe that as the number of neuronal connections increases, the ability of the structure to recognize individual classes of damage increases. However, achieving a precision of more than 99.8% requires the use of a much more extensive structure with a large number of convolution filters. However, it should be emphasized that the training time did not increase with increasing network parameters. This fact is related to the much simpler extraction of features from the input matrix with an increased number of filters. The elaboration of universal features contained in the input information by a CNN structure with a small

number of neural connections requires greater precision in the selection of the network’s weighting coefficients. Given this, the process is limited by the need to adjust the learning rate to values that allow for small changes in the weights of the network connections. This problem does not occur in structures with a much larger number of filters that enable the memorization of many features of the input matrix. Taking into account the implementation of CNN in programmable systems, it is crucial to provide as small several parameters as possible to ensure a high level of efficiency. Therefore, the adjustment of the precision threshold should be closely related to the task implemented by the neural structure.

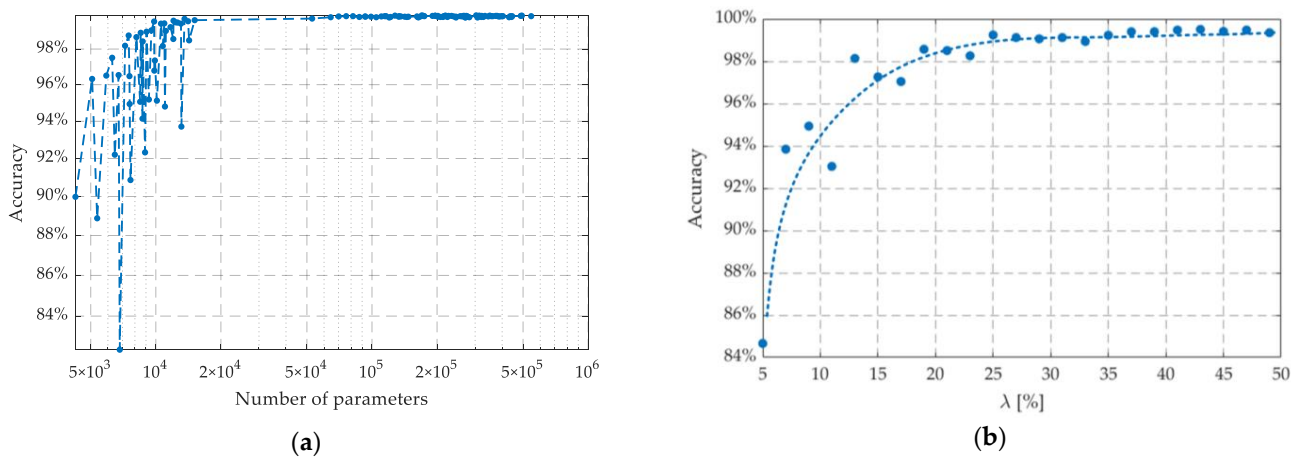


Figure 8. Dependency of network accuracy on (a) the number of its parameters and (b) the training set size: λ = training data size/training packet.

Table 5. Summary of selected CNN structures.

Assumed Accuracy	Achieved Accuracy	Convolutional Layers			CNN Learnable Parameters	Training Time [s]
		1 Layer	2 Layers	3 Layers		
90.0%	96.323%	20	20	40	5071	1281
92.0%	96.323%	20	20	40	5071	1281
94.0%	96.323%	20	20	40	5071	1281
96.0%	96.323%	20	20	40	5071	1281
98.0%	98.185%	20	40	60	7203	1246
99.0%	99.062%	20	60	80	9535	1212
99.5%	99.569%	20	80	60	9815	1279
99.8%	99.815%	80	20	20	64,413	1263
99.9%	99.908%	100	20	80	127,753	1256

In the neural calculations implemented, the network structures with a variable number of parameters in the range were analyzed: 4245–545,253. Of particular note, the highest precision of the neural structure (99.923%) was obtained for a network with 207,493 parameters, which is less than half of the analyzed range. Expanding the number of neural connections twice (545,253 parameters) did not result in such high precision (99.877%). Furthermore, increasing the number of parameters beyond 12,000 in the described diagnostic application resulted in a maximum increase in the classification precision of 0.25%. Therefore, increasing the network architecture should only be done up to a certain range, where a clear increase in efficiency due to an increase in the number of tuneable parameters is observable. In practical applications, the process of parameter selection is carried out while observing learning curves for the test data. Example waveforms of the curves for the structures described in Table 5 are shown in Figure 9.

The analysis of the learning curves shown in Figure 9 clearly shows a much higher level of precision of the diagnostic system based on extended structures. However, the analysis makes it possible to observe that regardless of the structure used, the training

process converges. As the number of neuronal connections increases, a reduced level of oscillation of the learning curves for testing data is noticeable. In addition, in the case of a reduced structure (red color), much lower dynamics of the learning process were observed. This means that the structure requires a larger number of epochs to tune the classifier parameters for the reduced number of diagnostic symptoms extracted from the convolution layers. The approximation shown in Figure 9 allows us to see that increasing the structures has an effect only up to a certain range, which confirms the results shown in Table 5.

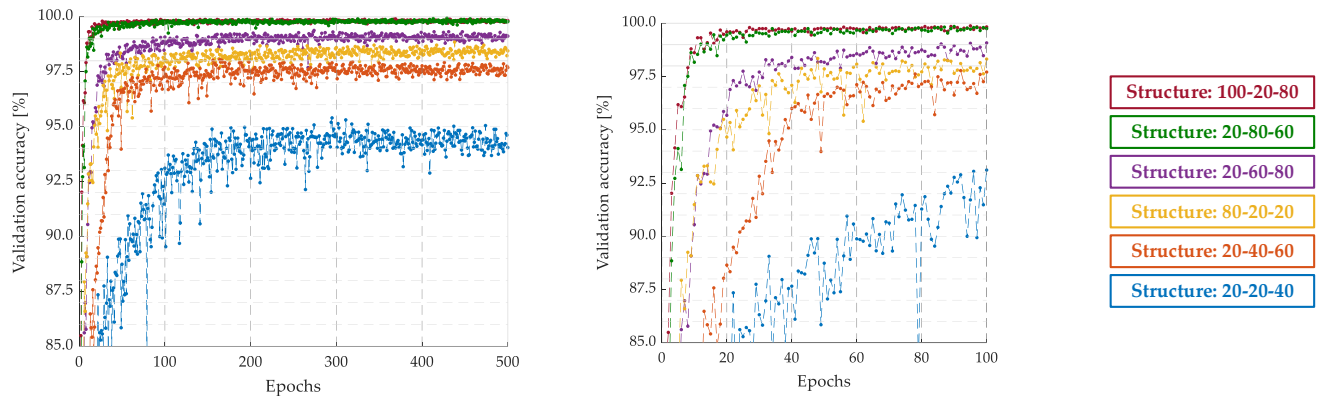


Figure 9. CNN training process—learning curves.

Concerning the importance of fault detection systems, the limitations associated with the use of CNNs should be noted. The implementation of CNNs in the diagnostic system results in difficulties in the form of a lack of formal rules for selecting hyperparameters for the structure and training process, the need for large learning datasets capable of providing automatic symptom extraction, the long process of training the network, the risk of losing its generalization capability, and the time to compute the response depending on the input information and network structure. However, these limitations were addressed in the study by optimizing the network structure and using the hyperparameter selection technique presented in [52]. Next, running the study on 1000 samples over a period, with a measurement lasting 10 s and a sampling rate of 50 kHz, yielded 500 cases from a single measurement, whereas using classical methods such as FFT would yield only one case; so, despite the need for a large training data set, it was simple and quick to develop. Further, the training process was optimized by using the SGDM algorithm based on mini-batches of data to average the gradient (speeding up the learning process, compared to classical approaches where usually the gradient is calculated for each sample separately), and the network training itself was performed using a GPU, giving a training time of slightly more than 20 min. Subsequently, the risk of losing the generalization of the network was eliminated through several approaches: the use of a stochastic learning technique (giving efficient exploration of the solution space and avoiding local minima), the analysis of learning curves for training and validation data (which helps verify that the model does not begin to over-fit the training data), and the use of a dropout layer (involving random resetting of the neuron weights, which forces the network to learn more elaborate and robust representations of the data). Finally, the study showed an average response time for the optimized network of 0.03 s. This time can be considered constant due to the constant size of the input matrix and the invariant number of operations performed on the network. Additionally, the network response was further accelerated by optimizing the structure, which in its smallest version has only 5071 parameters (with an accuracy of more than 96%, Table 5).

To verify the performance of CNN in fault diagnostic application, the next stage of the research concerns the analysis of the network's response to test packets containing samples obtained for the 13 classes. The responses of the developed neural structures were summarized in the form of confusion matrices shown in Figure 10.

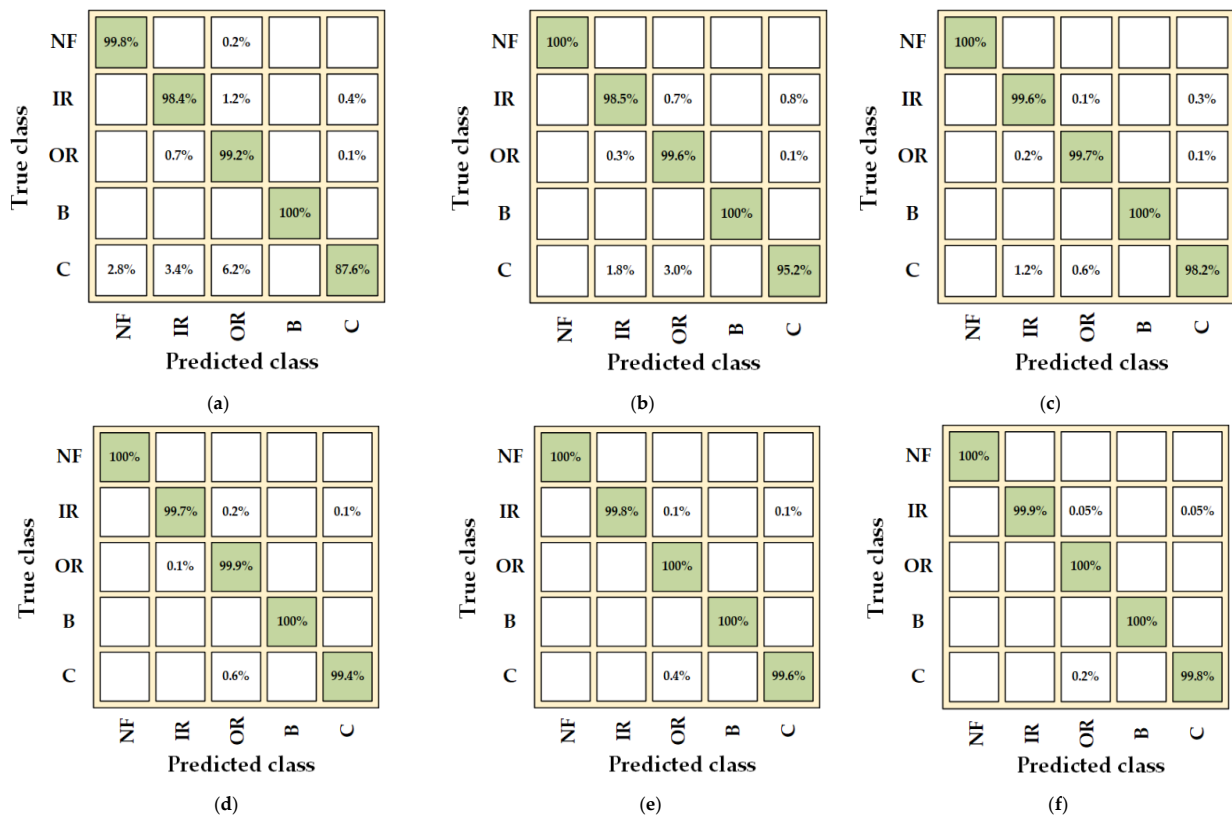


Figure 10. Verification of the proposed CNN structures—confusion matrix for different numbers of convolutional filter: (a) 20-20-40; (b) 20-40-60; (c) 20-60-80; (d) 20-80-60; (e) 80-20-20; (f) 100-20-80; NF—no fault, IR—inner race fault, OR—outer race fault, B—ball defect, C—cage defect.

The key task of diagnostic systems is to detect and evaluate the type of damage, while the precise determination of the degree of the defect is a secondary function. Therefore, in the first step, the responses of the network were analyzed in the form of division into each category of damage: inner race (IR), outer race (OR), ball (B), and cage (C). In the confusion matrices shown in Figure 10, the percentage effectiveness of the systems for each of the categories considered was represented. On this basis, the initial verification of the proposed structures was determined.

As can be observed in Figure 10, as the number of filters in each convolution layer increases, the proportion of false information obtained in the CNN output decreases. However, it should be emphasized that each of the structures presented, except for 20-20-40 (Figure 10a), was characterized by almost 100% defect detection precision, understood as the recognition between defect and no-defect states. Furthermore, an increase in the number of filters increased the effectiveness of the classification of the type of fault. Based on the analysis of the results shown in Figure 10, as well as the number of parameters of the structure (Table 5) and the analysis of the training process (Figure 9), it was decided that the 80-20-20 structure should be used in further studies. This network was characterized by a small number of parameters, a short weight adaptation time, and high detection and classification precision. To verify the selected structure, tests were carried out, including the classification of the type of defect and evaluation of the degree of rolling bearing degradation. The results obtained for different loads are shown in Figure 11.

The experimental verification of the developed detection system based on a deep neural network was carried out for defects of different kinds as well as degrees. As bearing damage cannot be modeled during drive operation, the course of mechanical vibration signals on the axis was artificially modeled by combining fragments of signals measured on the real object. As a result, it was possible to determine the response time of the neural structure to the occurrence of bearing damage.

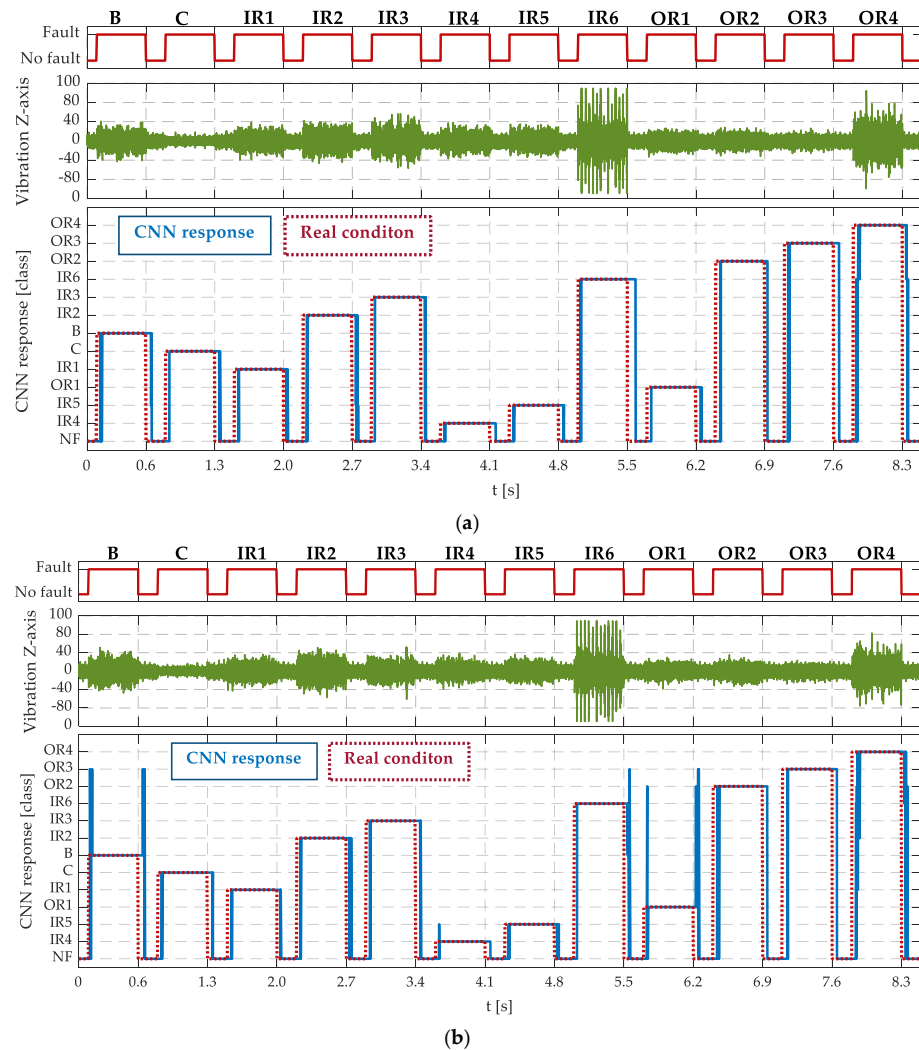


Figure 11. Verification of the proposed CNN structures (80-20-20): (a) $T_L = 0.5T_{LN}, f_s = 50$ Hz; (b) $T_L = T_{LN}, f_s = 50$ Hz.

The analysis of the results of the experimental verification shown in Figure 11 unambiguously confirms the high level of precision of the developed diagnostic method. The selected structure of the convolutional neural network is characterized by the high detection of damage and the assessment of the degree of fault. In addition, the short response time to an emerging defect is particularly notable, even in the case of damage at an early stage. Based on the analysis of CNN's response to the given input matrix, an average detection time of about 0.03 s was determined. As can be observed in Figure 11a, the response of the system is delayed concerning the moment the defect disappears. The fact is related to the presence in the input data buffer (data frame) of the samples characteristic of the damage state. Due to this, the neural structure still has information on part of the features attributable to the damage state. However, it should be noted that, from a practical point of view, damage decay does not occur and this study aimed to assess the response of CNN to dynamically changing input information. Only then is it possible to determine the response time, as well as the resistance to changes in the technical state of the bearing, and the operating conditions of the motor (load moment). The course of the network response, shown in Figure 11b, makes it possible to notice the false information about the technical condition of the bearings. An in-depth analysis of the CNN confirmed that the cause of the anomalies that appear is the previously described method of modeling mechanical vibrations. The use of a combination of diagnostic signal vectors results in the lack of an unambiguous response of the network when the input data buffer is half full of

samples characteristic of the fault condition and its absence. The response of the network determined by the probability of belonging to one of the categories is then ambiguous. However, in the practical implementation of the diagnostic system, such a situation will not occur.

5. Conclusions

The proposed diagnostic approach based on CNN's direct processing of mechanical vibration signals in rolling bearing diagnostics is an alternative to current methods that use advanced signal processing methods. Furthermore, the optimization of the neural structure allowed the reduction of the number of parameters to the necessary minimum, while ensuring a very high level of precision in the short time of damage detection and classification. In addition, the developed diagnostic system was characterized by a high sensitivity to a change in the degree of damage, so the application can be used in safety-critical systems. Future research will include an investigation into the applicability of current signals in rolling bearing damage diagnostics, which is not currently achievable using classical diagnostic methods such as the short-time Fourier transform, the Hilbert–Huang transform, etc. In addition, work on the application of a convolutional neural network in the diagnosis of bearing damage during transients (start-up, braking, and dynamic load changes) is planned to be carried out.

Author Contributions: Conceptualization, M.S. and M.D.; methodology, M.W. and O.F.; software, M.S. and J.J.J.; validation, M.S., J.J.J. and O.F.; formal analysis, M.D., K.S., S.W. and J.V.; data curation, M.W.; writing—original draft preparation, M.S., O.F. and J.J.J.; writing—review and editing, M.D., M.W., K.S., O.F., M.S. and A.W.; project administration, K.S., R.Z., M.D. and S.W. All authors have read and agreed to the published version of the manuscript.

Funding: Funded by the European Union under GA no 101101961—HECATE. The views and opinions expressed are, however, those of the author(s) only and do not necessarily reflect those of the European Union or Clean Aviation Joint Undertaking. Neither the European Union nor the granting authority can be held responsible for them. This project is supported by the Clean Aviation Joint Undertaking and its Members.

Data Availability Statement: Data are contained within the article.

Conflicts of Interest: Authors Sebastien Weisse and Jerome Valire was employed by the company SAFRAN Electrical & Power. The remaining authors declare that the research was conducted in the absence of any commercial or financial relationships that could be construed as a potential conflict of interest.

Appendix A

Table A1. Description and designations of the investigated damages.

Type of Damage	Label	Parameters
Rolling element	B	Spot indentation 0.5–1 mm deep
	C	Spot indentation 2 mm deep
Cage	IR1	Spot indentation 1 mm deep
	IR2	Spot indentation 1 mm deep
Inner race	IR3	Two spot indentations 1 mm deep
	IR4	Longitudinal scratch at a length of 3 mm
	IR5	Transverse scratch
	OR1	Spot indentation 1 mm deep
	OR2	Spot indentation 1 mm deep
Outer race	OR3	Two spot indentations 1 mm deep
	OR4	Longitudinal scratch at a length of 3 mm
	OR5	Transverse scratch
	NF	No fault

References

1. Xiong, R.; Sun, W.; Yu, Q.; Sun, F. Research progress, challenges and prospects of fault diagnosis on battery system of electric vehicles. *Appl. Energy* **2020**, *279*, 115855. [[CrossRef](#)]
2. Brelje, B.J.; Martins, J.R.R.A. Electric, hybrid, and turboelectric fixed-wing aircraft: A review of concepts, models, and design approaches. *Prog. Aerosp. Sci.* **2019**, *104*, 1–19. [[CrossRef](#)]
3. Nandi, S.; Toliyat, H.A.; Li, X. Condition Monitoring and Fault Diagnosis of Electrical Motors—A Review. *IEEE Trans. Energy Convers.* **2005**, *20*, 719–729. [[CrossRef](#)]
4. Bellini, A.; Filippetti, F.; Tassoni, C.; Capolino, G.-A. Advances in Diagnostic Techniques for Induction Machines. *IEEE Trans. Ind. Electron.* **2008**, *55*, 4109–4126. [[CrossRef](#)]
5. Gangsar, P.; Tiwari, R. Signal based condition monitoring techniques for fault detection and diagnosis of induction motors: A state-of-the-art review. *Mech. Syst. Signal Process.* **2020**, *144*, 106908. [[CrossRef](#)]
6. Singh, G.K.; Kazzaz, S.A.S.A. Induction machine drive condition monitoring and diagnostic research—A survey. *Electr. Power Syst. Res.* **2003**, *64*, 145–158. [[CrossRef](#)]
7. Li, Y.; Wang, H.; Li, J.; Tan, J. A 2-D Long Short-Term Memory Fusion Networks for Bearing Remaining Useful Life Prediction. *IEEE Sens. J.* **2022**, *22*, 21806–21815. [[CrossRef](#)]
8. Rubini, R.; Meneghetti, U. Application Of The Envelope And Wavelet Transform Analyses For The Diagnosis Of Incipient Faults In Ball Bearings. *Mech. Syst. Signal Process.* **2001**, *15*, 287–302. [[CrossRef](#)]
9. Stack, J.R.; Habetler, T.G.; Harley, R.G. Fault-signature modeling and detection of inner-race bearing faults. *IEEE Trans. Ind. Appl.* **2006**, *42*, 61–68. [[CrossRef](#)]
10. Luo, X.; Wang, H.; Han, T.; Zhang, Y. FFT-Trans: Enhancing Robustness in Mechanical Fault Diagnosis With Fourier Transform-Based Transformer Under Noisy Conditions. *IEEE Trans. Instrum. Meas.* **2024**, *73*, 2515112. [[CrossRef](#)]
11. Hoang, D.T.; Kang, H.J. A Motor Current Signal-Based Bearing Fault Diagnosis Using Deep Learning and Information Fusion. *IEEE Trans. Instrum. Meas.* **2020**, *69*, 3325–3333. [[CrossRef](#)]
12. Schoen, R.R.; Habetler, T.G.; Kamran, F.; Bartfield, R.G. Motor bearing damage detection using stator current monitoring. *IEEE Trans. Ind. Appl.* **1995**, *31*, 1274–1279. [[CrossRef](#)]
13. Caesarendra, W.; Kosasih, B.; Tieu, A.K.; Zhu, H.; Moodie, C.A.S.; Zhu, Q. Acoustic emission-based condition monitoring methods: Review and application for low speed slew bearing. *Mech. Syst. Signal Process.* **2016**, *72–73*, 134–159. [[CrossRef](#)]
14. Pandya, D.H.; Upadhyay, S.H.; Harsha, S.P. Fault diagnosis of rolling element bearing with intrinsic mode function of acoustic emission data using APF-KNN. *Expert Syst. Appl.* **2013**, *40*, 4137–4145. [[CrossRef](#)]
15. Yakkati, R.R.; Yeduri, S.R.; Tripathy, R.K.; Cenkeramaddi, L.R. Multi-Channel Time-Frequency Domain Deep CNN Approach for Machinery Fault Recognition Using Multi-Sensor Time-Series. *IEEE Access* **2023**, *11*, 116570–116580. [[CrossRef](#)]
16. Immovilli, F.; Bellini, A.; Rubini, R.; Tassoni, C. Diagnosis of Bearing Faults in Induction Machines by Vibration or Current Signals: A Critical Comparison. *IEEE Trans. Ind. Appl.* **2010**, *46*, 1350–1359. [[CrossRef](#)]
17. Patidar, S.; Soni, P.K. An Overview on Vibration Analysis Techniques for the Diagnosis of Rolling Element Bearing Faults. *Int. J. Eng. Trends Technol.* **2013**, *4*, 1804–1809.
18. Tandon, N. A comparison of some vibration parameters for the condition monitoring of rolling element bearings. *Measurement* **1994**, *12*, 285–289. [[CrossRef](#)]
19. Ewert, P.; Kowalski, C.T.; Orłowska-Kowalska, T. Low-Cost Monitoring and Diagnosis System for Rolling Bearing Faults of the Induction Motor Based on Neural Network Approach. *Electronics* **2020**, *9*, 1334. [[CrossRef](#)]
20. Liang, B.; Iwnicki, S.D.; Zhao, Y. Application of power spectrum, cepstrum, higher order spectrum and neural network analyses for induction motor fault diagnosis. *Mech. Syst. Signal Process.* **2013**, *39*, 342–360. [[CrossRef](#)]
21. Verstraete, D.; Ferrada, A.; Droguett, E.L.; Meruane, V.; Modarres, M. Deep Learning Enabled Fault Diagnosis Using Time-Frequency Image Analysis of Rolling Element Bearings. *Shock Vib.* **2017**, *2017*, 5067651. [[CrossRef](#)]
22. Ewert, P.; Kowalski, C.T.; Wolkiewicz, M. The application of wavelet analysis and neural networks in the diagnosis of rolling bearing faults in induction motors. *Przegląd Elektrotechniczny* **2013**, *89*, 124–127.
23. Filippetti, F.; Franceschini, G.; Tassoni, C. Recent developments of induction motor drives fault diagnosis using AI techniques. *IEEE Trans. Ind. Electron.* **2000**, *47*, 994–1004. [[CrossRef](#)]
24. Kowalski, C.T. *Diagnostyka Układów Napędowych z Silnikiem Indukcyjnym z Zastosowaniem Metod Sztucznej Inteligencji*; Oficyna Wydawnicza Politechniki Wrocławskiej: Wrocław, Poland, 2013.
25. Kowalski, C.T.; Orłowska-Kowalska, T. Neural networks application for induction motor faults diagnosis. *Math. Comput. Simul.* **2003**, *63*, 435–448. [[CrossRef](#)]
26. Ghate, V.N.; Dudul, S.V. Optimal MLP neural network classifier for fault detection of three phase induction motor. *Expert Syst. Appl.* **2010**, *37*, 3468–3481. [[CrossRef](#)]
27. Asfani, D.A.; Muhammad, A.K.; Syfaruddin; Purnomo, M.H.; Hiyama, T. Temporary short circuit detection in induction motor winding using combination of wavelet transform and neural network. *Expert Syst. Appl.* **2012**, *39*, 5367–5375. [[CrossRef](#)]
28. Hamdani, S.; Touhami, O.; Ibtouen, R.; Fadel, M. Neural network technique for induction motor rotor faults classification—dynamic eccentricity and broken bar faults. In Proceedings of the 8th IEEE Symposium on Diagnostics for Electrical Machines, Power Electronics Drives, Bologna, Italy, 5–8 September 2011.

29. Taibi, Z.M.; Hasni, M.; Hamdani, S. Optimization of the feedforward neural network for rotor cage fault diagnosis in three-phase induction motors. In Proceedings of the IEEE International Electric Machines & Drives Conference (IEMDC), Niagara Falls, ON, Canada, 15–18 May 2011.
30. Coelho, D.N.; Barreto, G.A.; Medeiros, C.M.S. Detection of Short Circuit Faults in 3-Phase Converter-Fed Induction Motors Using Kernel SOMs. In Proceedings of the 12th International Workshop on Self-Organizing Maps and Learning Vector Quantization, Clustering and Data Visualization (WSOM), Nancy, France, 28–30 June 2017.
31. Khalfaoui, N.; Salah, M.; Hamid Amiri, S. The SOM tool in mechanical fault detection over an electric asynchronous drive. In Proceedings of the 4th International Conference on Control Engineering & Information Technology, Hammamet, Tunisia, 16–18 December 2016.
32. Ghate, V.N.; Dudul, S.V. Cascade Neural-Network-Based Fault Classifier for Three-Phase Induction Motor. *IEEE Trans. Ind. Electron.* **2011**, *58*, 1555–1563. [[CrossRef](#)]
33. Gao, X.Z.; Ovaska, S.J.; Dote, Y. Motor fault detection using Elman neural network with genetic algorithm-aided training. In Proceedings of the IEEE International Conference on Systems, Man and Cybernetics 'Cybernetics Evolving to Systems, Humans, Organizations, and Their Complex Interactions', Nashville, TN, USA, 8–11 October 2000.
34. Goodfellow, I.; Bengio, Y.; Courville, A. *Deep Learning*; MIT Press: Cambridge, MA, USA, 2016.
35. Kao, I.-H.; Wang, W.-J.; Lai, Y.-H.; Perng, J.-W. Analysis of Permanent Magnet Synchronous Motor Fault Diagnosis Based on Learning. *IEEE Trans. Instrum. Meas.* **2019**, *68*, 310–324. [[CrossRef](#)]
36. Chattopadhyay, P.; Saha, N.; Delpha, C.; Sil, J. Deep Learning in Fault Diagnosis of Induction Motor Drives. In Proceedings of the Prognostics and System Health Management Conference (PHM-Chongqing), Chongqing, China, 26–28 October 2018.
37. Afrasiabi, S.; Afrasiabi, M. Real-Time Bearing Fault Diagnosis of Induction Motors with Accelerated Deep Learning Approach. In Proceedings of the 10th International Power Electronics, Drive Systems and Technologies Conference (PEDSTC), Shiraz University, Iran, 12–14 February 2019.
38. Mahesh, T.R.; Chandrasekaran, S.; Ram, V.A.; Kumar, V.V.; Vivek, V.; Guluwadi, S. Data-Driven Intelligent Condition Adaptation of Feature Extraction for Bearing Fault Detection Using Deep Responsible Active Learning. *IEEE Access* **2024**, *12*, 45381–45397. [[CrossRef](#)]
39. Kozma, R.; Ilin, R.; Siegelmann, H.T. Evolution of Abstraction Across Layers in Deep Learning Neural Networks. *Procedia Comput. Sci.* **2018**, *144*, 203–213. [[CrossRef](#)]
40. Ince, T.; Kiranyaz, S.; Eren, L.; Askar, M.; Gabbouj, M. Real-Time Motor Fault Detection by 1-D Convolutional Neural Networks. *IEEE Trans. Ind. Electron.* **2016**, *63*, 7067–7075. [[CrossRef](#)]
41. Li, C.; Xu, J.; Xing, J. A Frequency Feature Extraction Method Based on Convolutional Neural Network for Recognition of Incipient Fault. *IEEE Sens. J.* **2024**, *24*, 564–572. [[CrossRef](#)]
42. Shao, S.; Sun, W.; Wang, P.; Gao, R.X.; Yan, R. Learning features from vibration signals for induction motor fault diagnosis. In Proceedings of the International Symposium on Flexible Automation, Cleveland, OH, USA, 1–3 August 2016.
43. Principi, E.; Rossetti, D.; Squartini, S.; Piazza, F. Unsupervised Electric Motor Fault Detection by Using Deep Autoencoders. *IEEE/CAA J. Autom. Sin.* **2019**, *6*, 441–451. [[CrossRef](#)]
44. Han, S.; Sun, S.; Zhao, Z.; Luan, Z.; Niu, P. Deep Residual Multiscale Convolutional Neural Network With Attention Mechanism for Bearing Fault Diagnosis Under Strong Noise Environment. *IEEE Sens. J.* **2024**, *24*, 9073–9081. [[CrossRef](#)]
45. Wang, H.; Zhang, X. Fault Diagnosis Using Imbalanced Data of Rolling Bearings Based on a Deep Migration Model. *IEEE Access* **2024**, *12*, 5517–5533. [[CrossRef](#)]
46. Chen, Z.; Gryllias, K.; Li, W. Mechanical fault diagnosis using Convolutional Neural Networks and Extreme Learning Machine. *Mech. Syst. Signal Process.* **2019**, *133*, 106272. [[CrossRef](#)]
47. Pinedo-Sánchez, L.A. Vibration analysis in bearings for failure prevention using CNN. *J. Braz. Soc. Mech. Sci. Eng.* **2020**, *42*, 628. [[CrossRef](#)]
48. Eren, L.; Ince, T.; Kiranyaz, S. A Generic Intelligent Bearing Fault Diagnosis System Using Compact Adaptive 1D CNN Classifier. *J. Signal Process. Syst.* **2018**, *91*, 179–189. [[CrossRef](#)]
49. McNerny, S.A.; Dai, Y. Basic vibration signal processing for bearing fault detection. *IEEE Trans. Educ.* **2003**, *46*, 149–156. [[CrossRef](#)]
50. Randall, R.B. *Vibration-Based Condition Monitoring*; John Wiley & Sons: Hoboken, NJ, USA, 2011.
51. Magadán, L.; Roldán-Gómez, J.; Granda, J.C.; Suárez, F.J. Early Fault Classification in Rotating Machinery With Limited Data Using TabPFN. *IEEE Sens. J.* **2023**, *23*, 30960–30970. [[CrossRef](#)]
52. Skowron, M.; Kowalski, C.T.; Orłowska-Kowalska, T. Impact of the Convolutional Neural Network Structure and Training Parameters on the Effectiveness of the Diagnostic Systems of Modern AC Motor Drives. *Energies* **2022**, *15*, 7008. [[CrossRef](#)]

Disclaimer/Publisher's Note: The statements, opinions and data contained in all publications are solely those of the individual author(s) and contributor(s) and not of MDPI and/or the editor(s). MDPI and/or the editor(s) disclaim responsibility for any injury to people or property resulting from any ideas, methods, instructions or products referred to in the content.